Content:

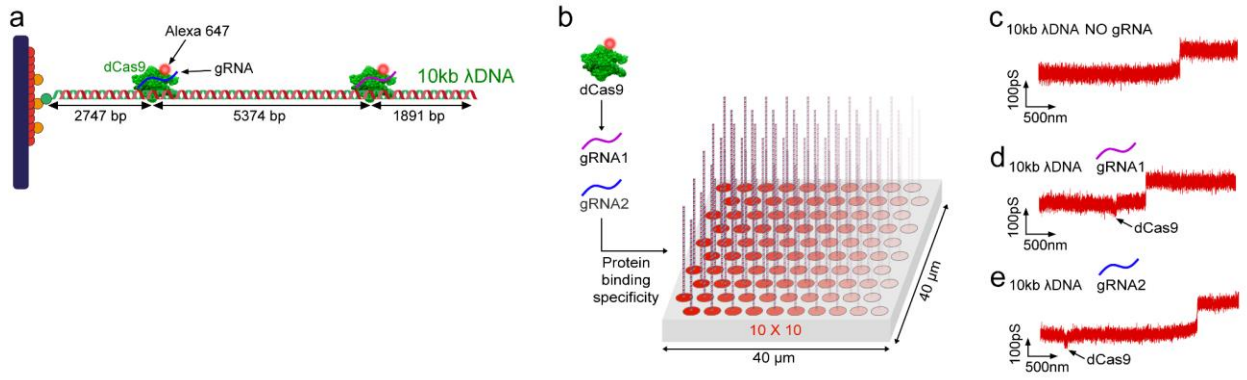

Supplementary Figure 1. Binding specificity of dCas9 on DNA with SICS. **a)** Design and construct of 10 kb long λ-DNA to test dCas9-DNA complexes with different RNA guides (gRNA). **b)** SICS mapping (10 × 10) of DNA-dcas9 complexes over a 40 x 40 μm^2 area detecting dCas9 binding specificity. In this proof-of-principle measurement, two gRNA were tested. **c)** SICS conductance-distance curve of a λ-DNA molecule translocated without dCas9/gRNA. **d)** Shows the detection of dCas9/gRNA1. **e)** Shows the detection of dCas9/gRNA2. These experiments were performed with 200 mV bias in 0.4 M KCl, pH=7.4.

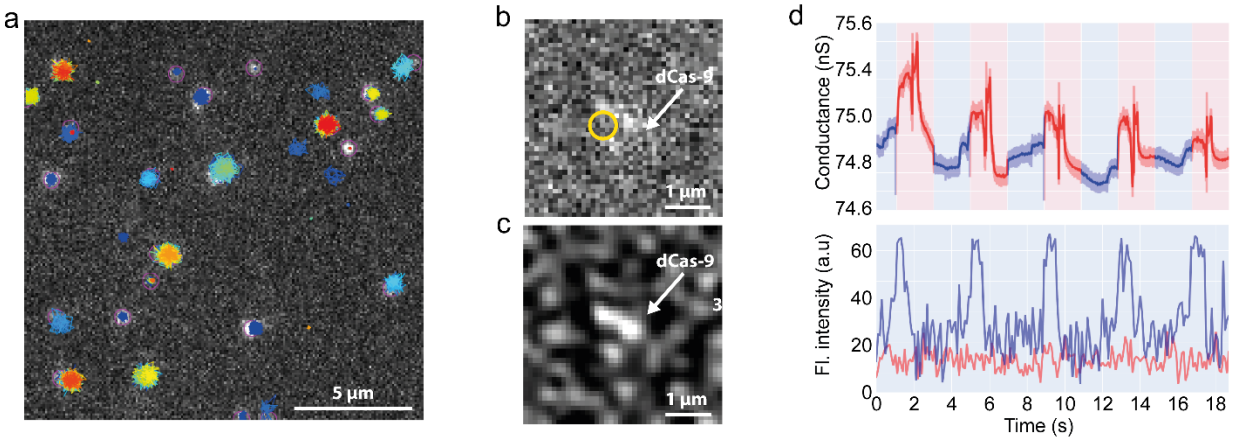

Supplementary Figure 2. Correlative single-molecule fluorescence and SICS measurement. A single widefield image showing the surface-immobilized DNA-dCas9 complex labeled with Alexa-647 dye. **a)** Single-particle tracks in different colors. **b)** DNA-dCas9 complex zoom-in. **c)** Band-passed image from (b) for improved visualization of the protein. **d)** A repetitive (n=5) correlative recording of conductance (top) co-aligned with fluorescence intensity (bottom) measured from the location marked in (b) plotted in blue and fluorescence intensity from the background plotted in red. The conductance signal is inverted in this plot. Light red shows a conductance recording at 0.01 samples/nm and dark red trace shows the signal with an average window of 1 nm. 5 approach-retract curves were acquired at the same spot marked in (b). The yellow circle marked in (b) also signifies the approach point of the glass nanopore. High concentration of free proteins used in the oxygen-scavenging system can influence the conductance signal in SICS, and cause sticking and clogging events.

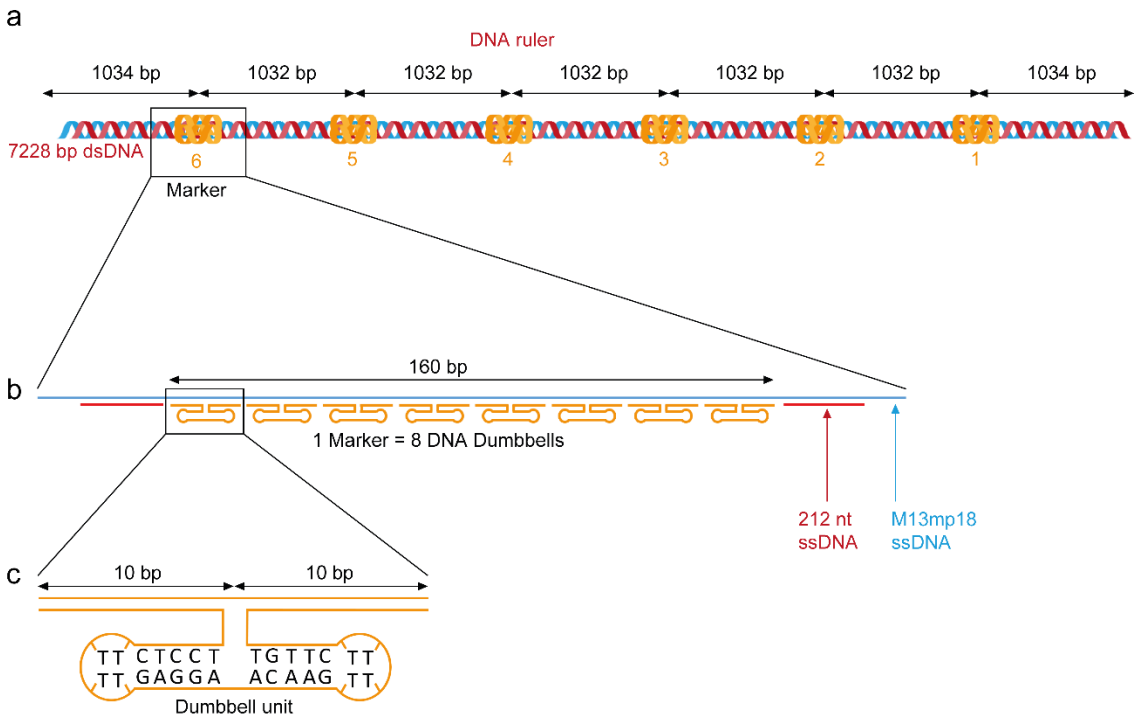

Supplementary Figure 3. Design of the DNA ruler construct. **a)** Schematic of a DNA structure composed of 7'228 base pairs in length with 6 markers separated by equal 1032 bp intervals. **b)** Each marker contains 8 DNA dumbbell hairpin motifs (in orange), which are joined to the backbone (M13mp18 in blue). The designed dumbbells and the complementary 212 ssDNA (in red) formed the final dsDNA ruler. (see methods section for more details). **c)** Base sequence of the dumbbell hairpin motif composed of two 10 bp sections.

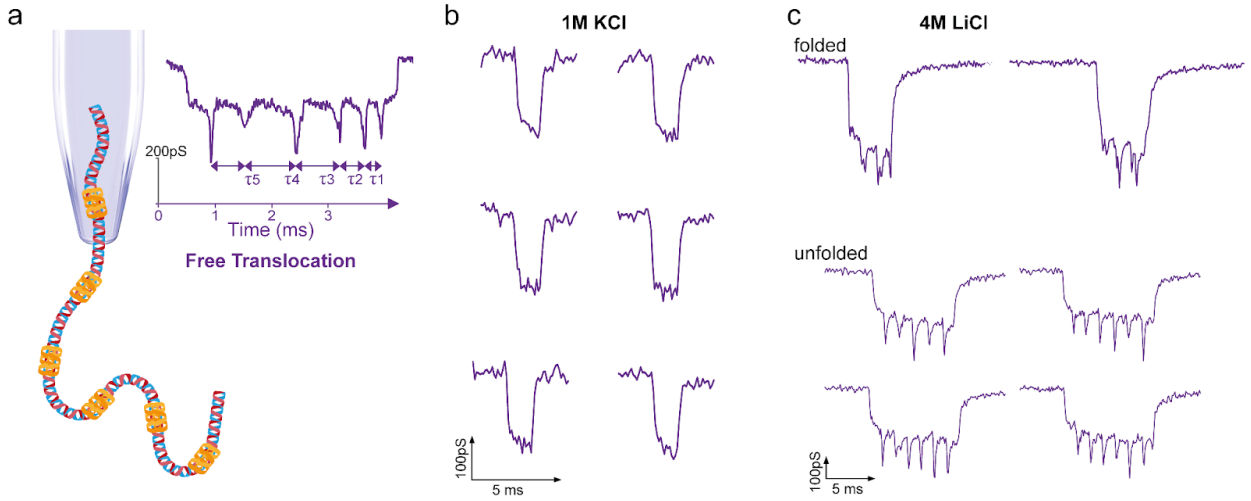

Supplementary Figure 4. Free translocation traces with glass nanopores of a DNA ruler with markers equally spaced along the DNA contour, highlighting the low detectability originated from the uncontrolled velocity. **a)** Schematic of a free-translocation of a molecule diffused in solution, with the corresponding signature that displays different velocity during translocation (different intra-event intervals τ). **b)** Free translocations in 1M KCl with 500 mV bias. **c)** Free translocations in 4 M LiCl. This figure highlights the challenges of free translocations in detecting topological features along DNA molecules with 600 mV bias. KCl medium has been shown to increase the SNR of the conductance signal compared with other salts (NaCl and LiCl)[13] but the translocation speed is too high to detect the features. 4M LiCl medium is typically a good alternative to slow down translocation speed, but the detection is still limited and translocations of folded molecules are recurrent (panel b - on top).

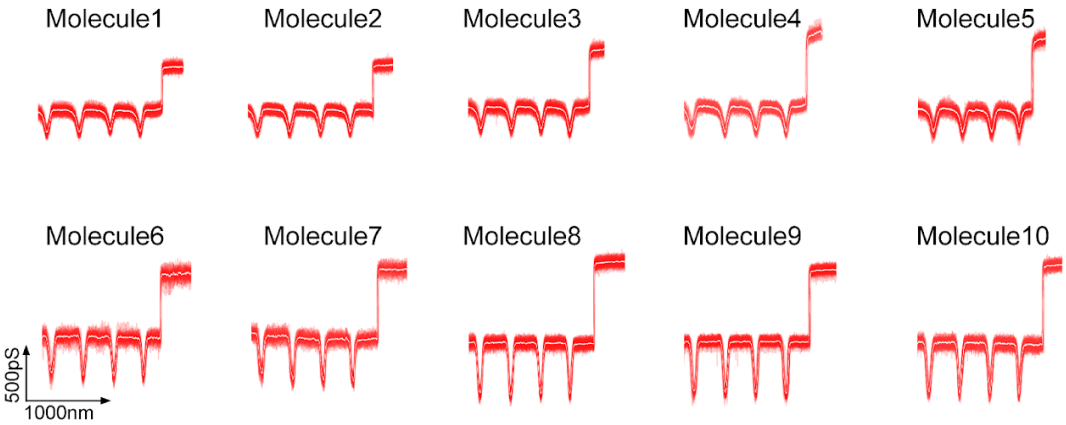

Supplementary Figure 5. Controlled translocation of 10 molecules, each scanned multiple times. The corresponding average of 10 curves generated in each molecule is shown in white (Averaged to 1 nm). Molecules were measured with several pipettes: Molecules 1 and 2 with a 16 nm radius pipette; Molecule 3 with a 14 nm radius pipette; Molecules 4 and 5 were acquired with a 13 nm radius pipette; 6 and 7 with a 10 nm radius pipette; 8, 9 and 10 with a 8 nm radius pipette. Light red shows a conductance recording at 0.01 samples/nm and dark red trace shows the signal with an average window of 1 nm.

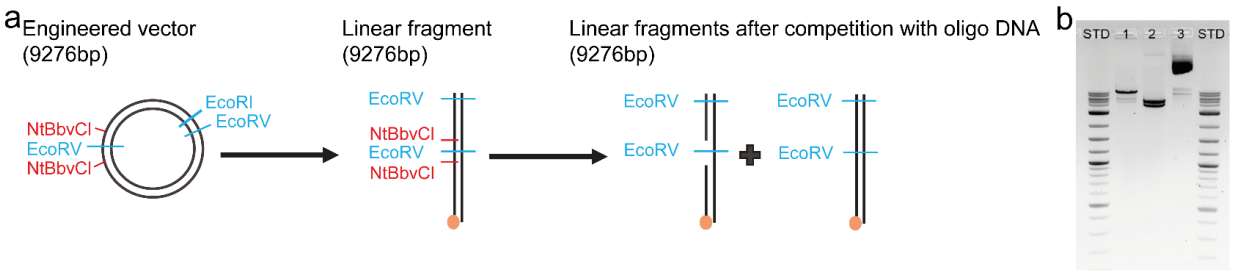

Supplementary Figure 6. Procedure for fustom-designed DNA gaps. **a)** We modified a 9 kb circular vector to introduce two Nt.BbvCI restriction sites flanking an EcoRV restriction site. First, the vector is linearized using digestion with EcoRI. Digestion with the nicking enzyme Nt.BbvCI introduces single-strand breaks in dsDNA and allows for subsequent elimination of the single-stranded DNA comprised between the nicks. The EcoRV site between Nt.BbvCI sites are used to eliminate ungapped molecules. Indeed, upon successful gap formation, EcoRV will not recognize the (now single-stranded) restriction site. In contrast, if gap formation fails and the fragment remains ungapped, digestion with EcoRV will generate two fragments of smaller sizes that can easily be eliminated. **b)** Construct characterization using electrophoresis on an agarose gel. Lane 1: Biotinylated, gapped DNA purified, after additional digestion with EcoRV. Additional digestion with EcoRV cannot cut DNA at the gap because EcoRV only hydrolyzes double-stranded DNA. Thus, the ~9kb fragment is left intact. There might still be a minority fraction of fragments that do not contain the gap which gives rise to two smaller linear fragments (see two faint bands below the main band). Lane 2: If the engineered vector is digested with EcoRV before gap formation, it produces two linear fragments, (that appear like a single, thick band on the picture), as expected. Lane 3: Undigested engineered vector.

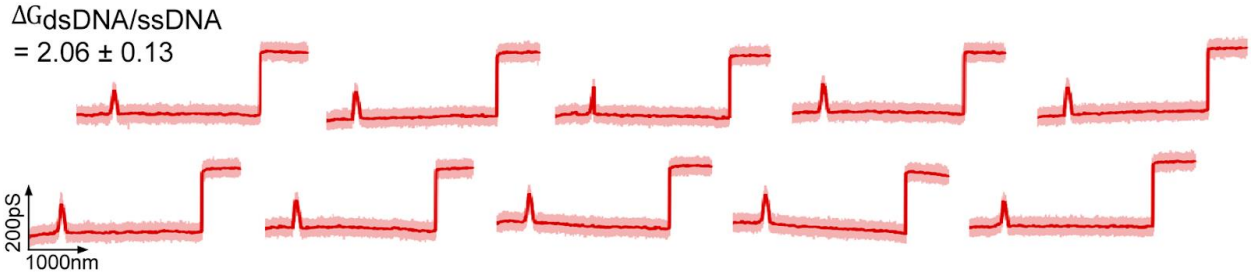

Supplementary Figure 7. Ratio of the dsDNA to ssDNA conductance change for translocations on 80 nt DNA gaps. Light red shows a conductance recording at 0.01 samples/nm and dark red trace shows the signal with an average window of 1 nm. N=10.

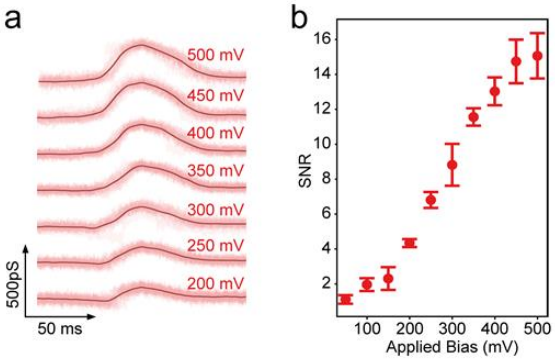

Supplementary Figure 8. SICS translocation of the DNA gap construct containing the 80 nt gap, with a tunable bias for a constant speed of 1 μm/s. **a)** SICS curves with a 13 nm radius pipette. In dark red is the average of 10 curves for each bias, and in light red is the overlay of 10 curves, at 0.01 samples/nm. **b)** SNR of averaged translocations vs applied bias. The error bars represent the standard deviation and the center is the mean SNR of the same detected gap at different bias, $N = 10$ for each bias.

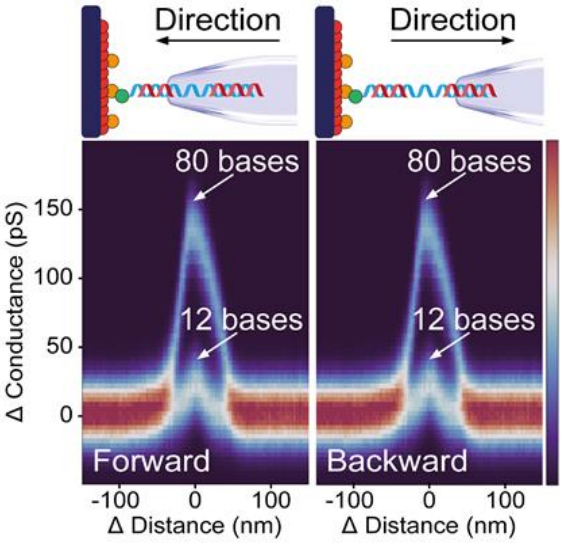

Supplementary Figure 9. Bidirectional readings with SICS. This figure shows the color-coded probability density map (n=100 curves) of forward (left panel) and backward (right panel) controlled-translocations curves of 80 nt and 12 nt DNA gaps at 1 μm/s translocation velocity with 12 nm radius pipette, 0.01 samples/nm, N = 100;. The colormap represents the normalized probability of occurrence for a conductance value at a corresponding distance, 0 – 0.8 range. The capability to have control over the pulling directionality allowed us to observe DNA hairpins at 4 °C see SI Figure 15.

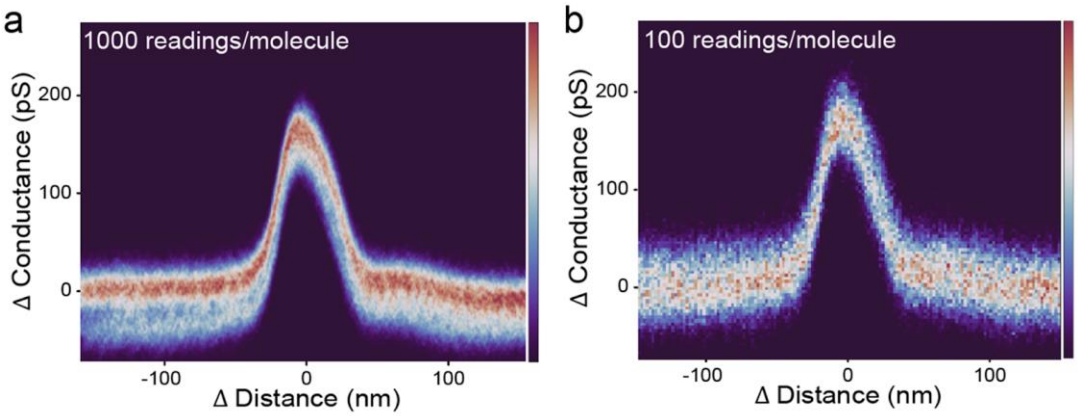

Supplementary Figure 10. Probability density map on the same 80 nucleotide gap. **a)** 1000 readings/of the same single-molecule molecule. **b)** 100 readings/of the same single-molecule. The linear colormap represents the normalized probability of occurrence for a conductance value at a corresponding distance, 0 – 1 range. 10 nm glass nanopore radius at 1 μm/s translocation velocity, signal average window of 1 nm.

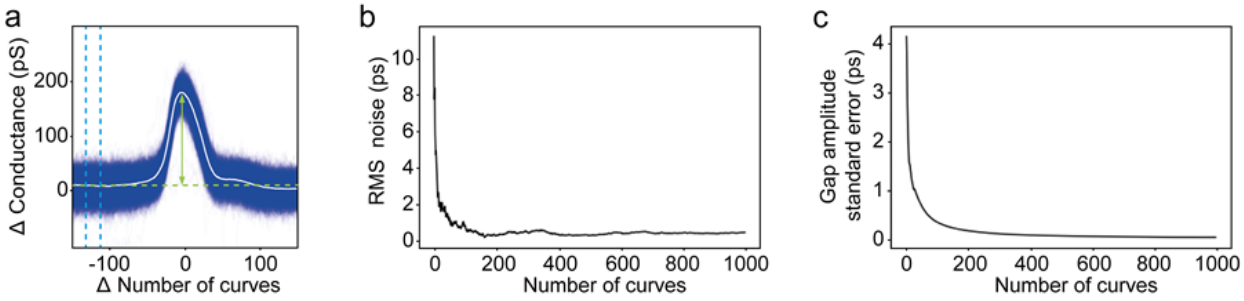

Supplementary Figure 11. Improvement of the translocation SNR and detection of amplitude error by averaging multiple traces from the same feature on the same molecule. **a)** Average of 1000 curves on the same 80 nt gap at 1 μm/s translocation velocity, recording 0.01 samples/nm with 10 nm radius pipette and 300 mV bias in 1 M KCl. **b)** RMS noise measured in 20 nm range, blue dashed lines in panel (a). **c)** Standard error of the detected gap amplitude, green arrows in panel (a).

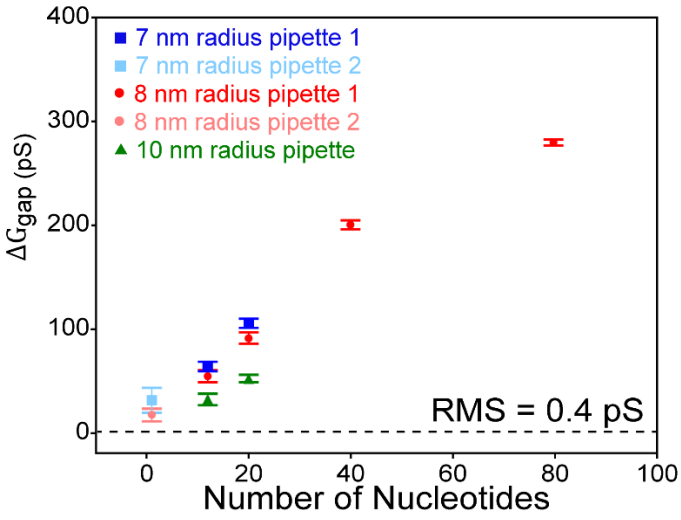

Supplementary Figure 12. Amplitude of the detected gaps (ΔGgap) vs gap length (in nucleotides) with different pipettes represented in different colors. The error bars represent the standard deviation and the center is the mean amplitude of the detected gap (N = 40 for 7 nm radius pipette 2, and N = 10 for the other pipettes).

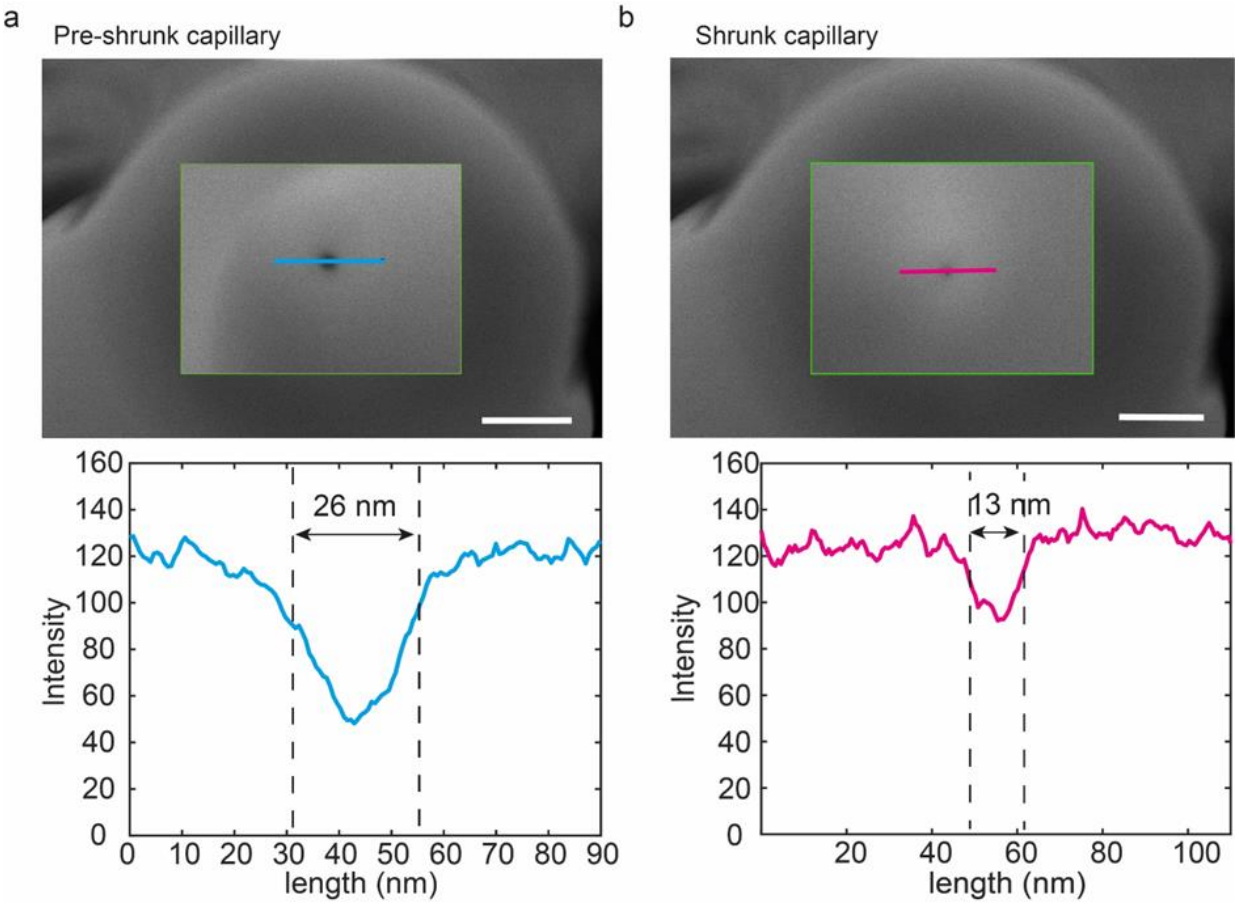

Supplementary Figure 13. Shrinking procedure and pore radius measurement. **a)** Pre-shrunk capillary and **b)** Shrunk capillary with their respective intensities across the pore. The pore edge is defined as the point where the intensity drops to 80% of the baseline intensity value. Scale bars = 100 nm.

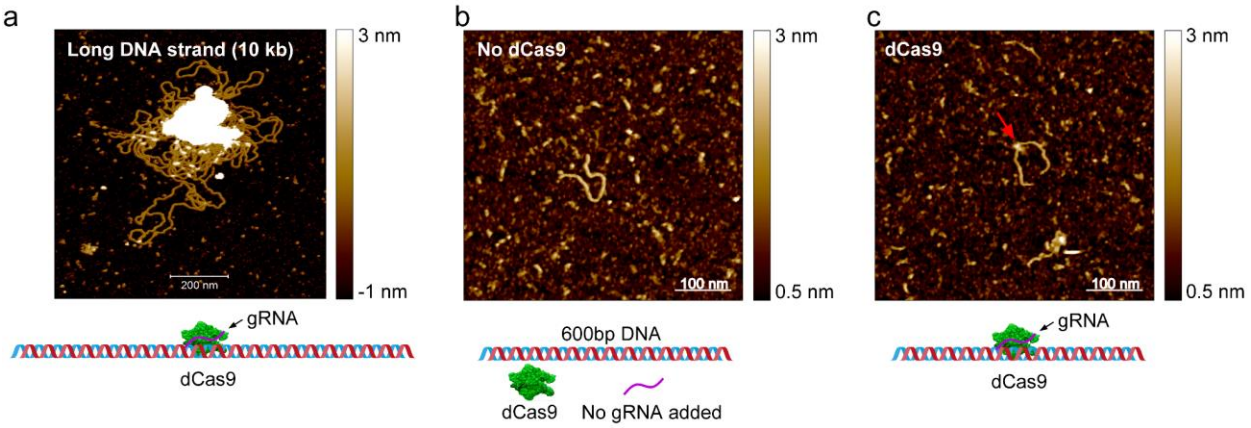

Supplementary Figure 14. Atomic force microscopy imaging of DNA-dCas9 complex. **a)** AFM image of 10 kb long DNA incubated with dCas9 and gRNA, demonstrating that AFM analysis is not feasible on long DNA molecules. **b)** A negative control experiment with an absence of gRNA with no observed dCas9 binding. **c)** A positive control, with gRNA present in a solution with a dCas9 binding event in a field-of-view (red arrow).

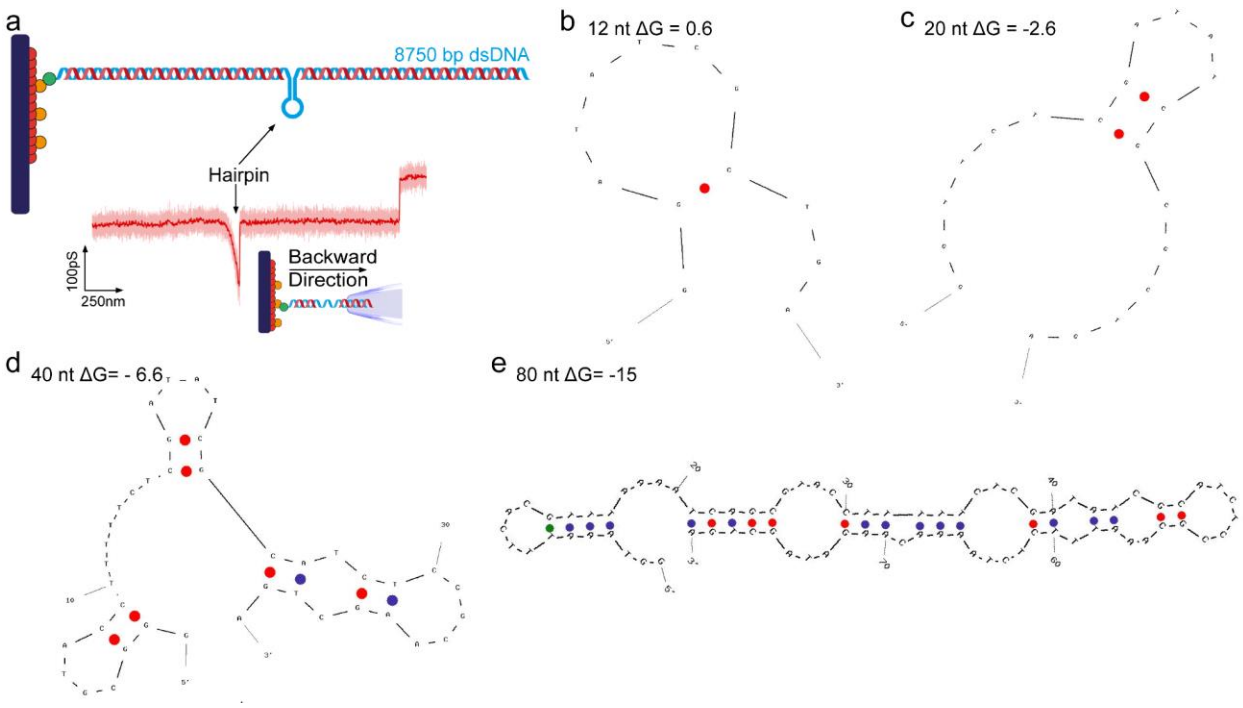

Supplementary Figure 15. Hairpin formation in DNA gap molecules. **a)** Design of a DNA gap construct (40 nt gap) with the formation of a hairpin and a SICS conductance-distance curve in red. Light red shows a conductance recording at 0.01 samples/nm and dark red trace shows the signal with an average window of 1 nm. Prediction of secondary structures and Gibbs free energy values (ΔG) at 4°C for the sequences of the single-strand DNA stretch in four DNA gap constructs: 12 nucleotide gap **b)**, 20 nucleotide gap **c)**, 40 nucleotide gap **d)**, and 80 nucleotide gap **e)**. This figure highlights the formation of hairpins that were observed during SICS experiments, in samples measured right after incubation at 4°C. The experiments were performed with 300 mV bias in 1 M KCl. The bidirectional capability of SICS (SI Figure 9) is relevant in this application as it allows us to exploit the balance between drag and electrophoretic force. Decreasing the total force acting on the molecule in the backward direction allowed us to observe a prominent peak (a) that we assigned to the hairpin formation. In forward direction, the total force is high enough that our data are similar to the results shown in the main figures after samples have been brought to room temperature (Figure 3 and 4).

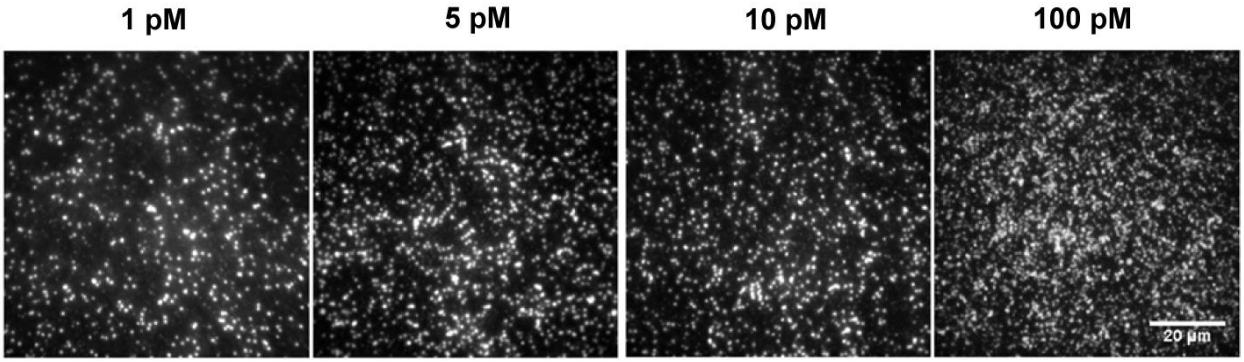

Supplementary Figure 16. Imaging of DNA tethered on a glass coverslip with a widefield fluorescence microscope. The different BSA-Bt tether concentrations indicated above (1, 5, 10, 100 pM). 100 pM DNA solution and 5 nM YOYO-1 dye was used for all experiments. DNA surface densities were calculated using a single-molecule localization approach. DNA surface density values were found to be (from left to right): 0.09, 0.22, 0.24, 0.44 DNA molecules per μm^2.